Precise Timing Based on Pulsar Observation for Grid Synchronization

Xiqian Luo[1], He Yin[1], Wei Qiu[1], Liang Zhang[1], Yilu Liu[1, 2]
[1]Department of Electrical Engineering and Computer Science, The University of Tennessee, Knoxville, TN, USA
[2]Oak Ridge National Laboratory, Knoxville, TN, USA
{xluo18, hyin8, wqiu4, lzhan104, liu}@utk.edu

2021 IEEE Power & Energy Society Innovative Smart Grid Technologies Conference (ISGT) | 978-1-7281-8897-3/21/$31.00 ©2021 IEEE | DOI: 10.1109/ISGT49243.2021.9372160

***Abstract*—While Global Positioning System signals are widely used as the synchronized timing sources for wide-area measurement systems for power grid monitoring and control, they are vulnerable to failures and malicious attacks. To address this problem, an alternative kind of timing sources, the millisecond pulsars, were proposed to serve the power grid as they are more precise and physically indestructible. Millisecond pulsars are a kind of neutron stars that emit radio pulse signals that have extremely stable periods of milliseconds. However, the observed pulse signals from pulsars cannot be directly used for timing because of their low signal-to-noise ratio and the dispersion effects of interstellar medium. In this paper, the precise timing method based on pulsar observation data is proposed to interpret the pulsar observation data and therefrom to generate precise timing signal for the power grid synchronization. In our proposed method, incoherent de-dispersion is used on the observation data to mitigate the effect of interstellar medium dispersion. Then spectrum analysis and segment folding are used to precisely estimate the local pulsar period. Finally the standard pulse per second signal is generated from the estimated pulsar period and its precision is analyzed. Experiments with the observation data of the pulsar J1939+2134 show that the generated pulsar based timing signal can be more accurate compared to GPS timing signals.**

***Index Terms*—grid synchronization, timing source, pulsar, folding, period estimation**

I. Introduction

With the increasing scale of power grids and the penetration of distributed renewable sources, power grids have become more complex and dynamic. Therefore, a real-time wide area monitoring, protection and control system is crucial for ensuring the secure and reliable operation of the power systems [1]. Wide-area measurement system (WAMS), which is based on synchronized data from phase measurement units (PMU), has been utilized to complement the traditional supervisory control and data acquisition (SCADA) system to improve operator's situation awareness [2]. It is able to deliver fast and proactive grid stability management to meet the complex challenges of modern power systems.

Since WAMS is based on real-time synchrophasors, time synchronization is crucial to operation of WAMS [3]. Global Positioning System (GPS) signals are widely used as the timing sources for synchronization for wide-area monitoring, protection and control systems in power grid. However, GPS signals are not reliable because they are susceptible to a number of factors, such as system failures, space weather change, jamming. Meanwhile, the cyber attacks, e.g. GPS spoofing, will cause tremendous measurement errors to the WAMS [4]. Therefore, a more secure and stable timing system is required.

Pulsar-based timing was first proposed as a potential alternative timing source for grid synchronization in [5], [6]. Pulsars are a kind of rotating neutron stars that emit radio pulses at extremely stable intervals from milliseconds to seconds [7]. For some pulsars that have periods of several milliseconds, which are termed as Millisecond Pulsars (MSPs), the periods of their pulse signal are almost as stable as terrestrial atomic clock. For example, the 5.75-ms pulsar J0437-4517 yields a root mean square residual between measured and model arrival times of about 100ns over an observing time of one year or longer [8]. Besides, pulsars have long-term stability that extends to millions of years, considerably longer than terrestrial atomic clocks [9]. Further, as neutron stars in the universe, pulsars can be observed worldwide and are physically indestructible. Hence, the pulsars can serve as a highly stable and repeatable timing sources for grid synchronization.

The periodic pulse signals that the pulsars emit can be observed by radio telescopes. However, pulsars are weak radio sources, and their flux densities are relatively low and fluctuating with time [7]. It makes the pulses indiscernible with noise and interference. Besides, during the transmission, the pulse signals are affected by the frequency-dependent transmission speed in the interstellar medium, which results in dispersion in the received observation data and degrades the time resolution of the pulse signal [7]. As a result, it is impossible to use the pulse signals for timing directly. These two problems, the low and fluctuating flux density problem and the dispersion problem, need to be solved when using pulsar observation data for timing. Signal processing is necessary to detect and recover the pulse signals from distortion, noise and interference.

In this paper, the precise timing method based on pulsar observation is proposed to process and interpret pulsar observation data for timing in grid synchronization. Incoherent de-dispersion is used to mitigate the dispersion, and segment

This work was supported primarily by the Major Research Instrumentation Program of the National Science Foundation under NSF Award Number ECCS-1920025.

This work made use of Engineering Research Center shared facilities supported by the Engineering Research Center Program of the National Science Foundation and the Department of Energy under NSF Award Number EEC-1041877 and the CURENT Industry Partnership Program.

978-1-7281-8897-3/21/$31.00 ©2021 IEEE

folding is proposed to precisely estimate the period of the pulse signals. Further, the method to generate precise timing signals is proposed and analyzed. Using an observation data instance of one pulsar, J1939+2134, it is proved that our proposed methods can process the dispersed low signal-to-noise ratio (SNR) observation data and generate timing signals with error of 10^{-8}, which is more accurate than GPS timing signals. The generated timing signal can serve as an reliable alternative and supplementary timing source in WAMS and for grid synchronization.

The main contributions of our work can be summarized as follows:

- The method to estimate the local period of the pulsar from the dispersed observation data is proposed, in which spectrum analysis is used for coarse estimation and segment folding is used for fine estimation.
- The method to generate pulse per second (PPS) signal based on local clock and the local period estimate of the pulsar is proposed, and its accuracy is analyzed.

II. Preliminaries

A. Dispersion

Dispersion is one of the problems that challenges the pulsar-based timing. When the radio pulse signals that one pulsar emits travel through the interstellar medium in space, pulses emitted at higher frequencies travel faster than their counterparts at lower frequencies and thus arrive earlier at the earth, as shown in Fig. 1. This phenomena is called dispersion. For a certain pulsar, the travel time of pulses emitted at frequency f is given by

$$t = t_0 + \frac{\mathrm{D}}{f^2} \times \mathrm{DM}, \tag{1}$$

where D is the dispersion constant that is $\mathrm{D} \approx 4.1488 \times 10^3\,\mathrm{MHz}^2\,\mathrm{pc}^{-1}\,\mathrm{cm}^3\,\mathrm{s}$, and DM is the dispersion measure (DM) of each pulsar that is stable and can be looked up in the database for any known pulsars [10].

The received pulses are dispersed, that is, much wider than their original shape, as shown in Fig. 1. The widened pulse degrades the time resolution of the pulse signal. When the DM is large or when the observation frequency range is broadband, dispersion may even make the pulses indistinguishable. As a result, the effect of dispersion must be mitigated to observe the clear pulse signals of the pulsars.

There are two kinds of de-dispersion methods, incoherent and coherent ways [7]. In incoherent de-dispersion, pulse signals are divided into filterbank channels and then the signals of each filterbank channel are aligned to mitigate the dispersion. Delays between filterbank channels are mitigated, but the delay within each channel are not processed. In coherent de-dispersion, the dispersion is totally mitigated with a phase filter, but it is computational expensive. Incoherent de-dispersion is simpler and more efficient, and is enough for pulsars with dispersion measures that satisfy $\mathrm{DM} < 100$. In this paper, incoherent method is used for de-dispersion, which will be detailed in Section III.

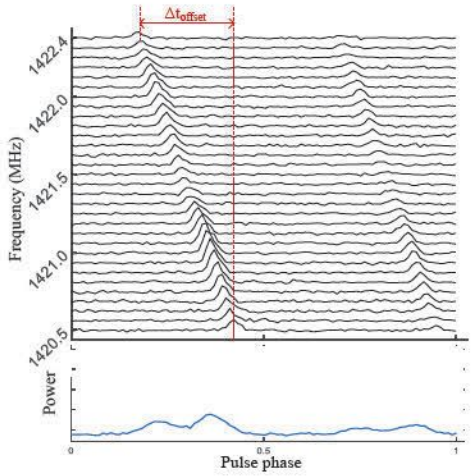

Fig. 1. Pulses at different frequencies and summed pulse profiles with effect of dispersion.

B. Folding and integrated pulse profile

Considering the weak flux density of the pulsar and the constraint of telescope sensitivity, one single pulse that the pulsar emits is hard to observe. As a result, it is impossible to use the pulse signal directly for timing. To observe the pulses that the pulsar emits, the solution in radio astronomy is to coherently add many pulses together, hundreds or even thousands, to make the pulse discernible from noise. This is called folding. If a pulse signal is folded with its correct period, it will form a particular integrated pulse profile. For each pulsar, its integrated pulse profile is stable and unique, like its 'fingerprint'.

To get the integrated pulse profile, the key point is to fold the signal with the correct pulse period. For any known pulsar, its period is known. But considering that the clock at the telescope is not a standard clock, the period measured by the local clock must be estimated before implement folding. Let us denote the pulsar period measured by the local clock as local period P_l and the period measured by standard time as standard period P_s. Once the local period P_l is estimated, the relationship between local clock and standard time can be calculated as follows

$$P_l * 1\,\text{unit local time} = P_s * 1\,\text{unit standard time}. \tag{2}$$

According to (2), the local clock can be adjusted and corrected to generate the standard timing signal.

The correct estimation of local period is crucial to the integrated pulse profile. When there exists error between the true value and the estimate value of the local period used in folding, pulses are not aligned and the position of each pulse will drift to get a widened pulse profile. According to this fact, segment folding is proposed to estimate the precise local period in Section III.

III. Pulsar Observation Data Process

Although the pulsars have very stable periods as reliable timing sources, the relative low and fluctuating flux densities

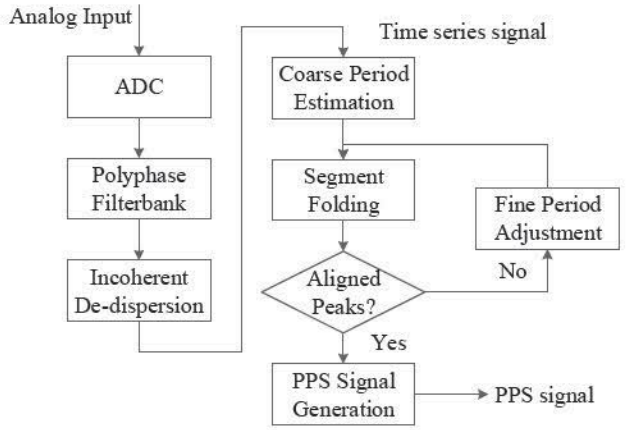

Fig. 2. Block diagram of pulsar data processing

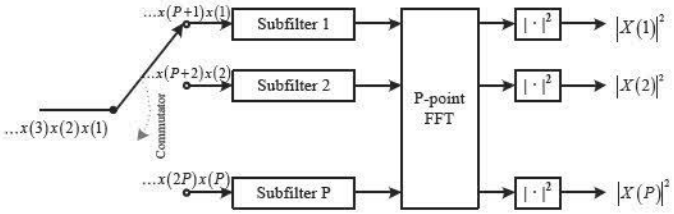

Fig. 3. Structure of Polyphase Filterbank spectrometer

and the influence of the interstellar medium (ISM) make the pulse signals hard to observe. In this section, we proposed the method to interpret pulsar observation data and to generate accurate timing signals. The whole processing procedure is depicted in Fig. 2, which starts from the output of ADC in the radio telescope and ends at the generation pulse per second (PPS) signals.

The analog inputs of the ADC are the raw voltages the radio telescope detects that have been down-conversed to baseband. The outputs of ADC is the digitized samples of the pulse observation data. First, the data are incoherently de-dispersed with a polyphase filterbank (PFB) block and an incoherent de-dispersion block. The de-dispersion data are feed to the coarse period estimator and the result goes to the folding part. Then at the folding stage, the segment folding block and the fine period adjustment block form a close-loop with feedback. With an estimation of period, the dispersed time series data are folded to get integrated pulse profiles. By detecting the peak position of the integrated pulse profiles, the estimation of the period can be adjusted. Once the accurate estimation of period is obtained, we can generate the standard time PPS with local clock according to the estimate of local period.

In this section, the details of each step will be discussed.

A. PFB and incoherent de-dispersion

The Polyphase filterbank (PFB) block divides the pulse signal data into separate filterbank channels, while the incoherent de-dispersion block align the data of each channel according to the DM.

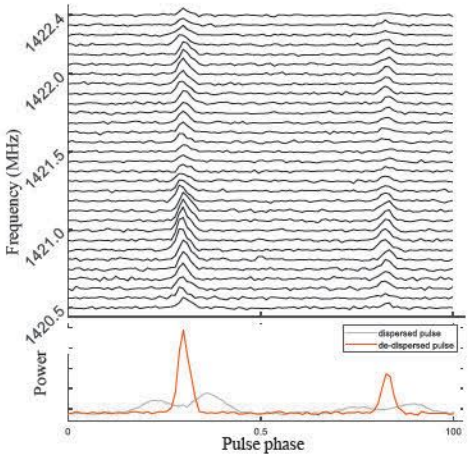

Fig. 4. Pulses at different frequencies and summed pulse profiles after incoherent de-dispersion (red line), compared with the pulse profile before de-dispersion (gray line).

PFB is a digital spectrometer that can get the spectrogram of the input signal, which shows its spectrum of frequencies as it varies with time. It first implements FFT to the time signal and then squares the frequency response to get the spectrum. But instead of doing FFT directly to a truncated time signal, PFB adds a windowing filter before FFT to ameliorate the spectral leakage and thus gets a better performance. As shown in Fig. 3, PFB consists three parts: 1) the PFB frontend to filter the input data with the windowing functions, 2) the P-point Fast Fourier Transform (FFT) and 3) the square part to get the power spectrum. The PFB frontend uses a polyphase filter for windowing, which includes P subfilters. Through PFB, the raw voltage data are divided into P filterbank channels, and the power data of each channel that vary with time are get.

Then the pulse at each channel is aligned in the incoherent de-dispersion block, as shown in Fig. 1 and 4. Propogation delayed for the i-th filterbank channel centered at frequency f_i is given in (1). Compared with the first channel whose center frequency is f_0, the relative time offset of the i-th channel is

$$\Delta t_i = \mathrm{D} \times \mathrm{DM} \times \left(\frac{1}{f_0^2} - \frac{1}{f_i^2}\right). \tag{3}$$

To compensate the time offset, data at the i-th channel is delayed the by Δt_i.

After the alignment, the power data at each channel are added together and form a time series that has been de-dispersed. As a result of PFB, the sampling period compared with the raw data out from ADC degrades by P times. For raw voltage data that have period of $t_{\mathrm{org\_smp}}$, the time series after incoherent de-dispersion is $t_{\mathrm{smp}} = P \times t_{\mathrm{org\_smp}}$.

B. Spectrum Analysis and coarse period estimation

When folding the time series after de-dispersion, we may need to fold hundreds or even thousands pulses to make the pulse discernible. However, the longer series we folded, the more sensitive is the resulting integrated profile to the estimation error of the pulse period. This makes initialization

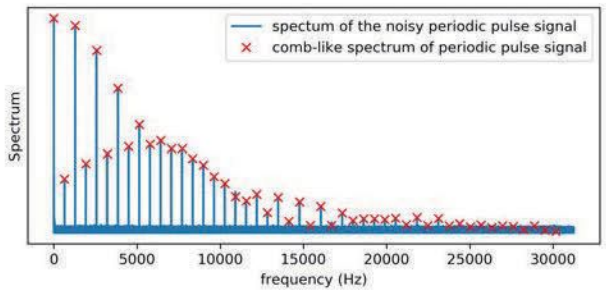

Fig. 5. Spectrum of the noisy periodic pulse signal

of the pulse period estimation based on folding difficult. As a result, spectrum analysis is proposed to get a initial coarse estimate of the local pulsar period.

The spectrum analysis is based on the fact that periodic pulse signal has different spectrum structure compared to white noise. The periodic pulse signal can be modeled as the convolution of a single pulse $s(t)$ and a sampling function with period T as

$$s(t) = x(t) * \sum_m \delta\left(t - mT\right) = \sum_m x\left(t - mT\right), \quad (4)$$

and its spectrum is the multiplication of $X(f)$, which is the spectrum of $x(t)$, and the spectrum of the sampling function, which is comb-like, as

$$S(f) = X(f) \sum_m \delta\left(f - \frac{m}{T}\right) = \sum_m P(\frac{m}{T}) \delta\left(f - \frac{m}{T}\right). \quad (5)$$

As a result, the spectrum of the periodic pulse signal is a weighted comb-like function. In the meantime, the noise is continuous over the whole bandwidth. The spectrum of the periodic pulse signal and noise can be easily separated when spectrum analysis is implemented to signal of a long enough period of time, as shown in Fig. 5. From (5), the intervals between the teeth of the weighted comb-like spectrum is $1/T$. So a coarse estimate of the pulse period T could be obtained by measuring the average gap between the teeth of the weighted comb-like spectrum.

Input of the coarse period estimate is the discrete time series out from the de-dispersion block with sampling period as t_{smp}. To do spectrum analysis, FFT is implemented to the first $N = 2^k$ points. Given the frequency interval between spectrum bins is $\frac{1}{Nt_{\text{smp}}}$, the average gap between the teeth of the comb-like signal spectrum can be calculated to be the estimate of $1/\hat{P}_l$.

C. Segment folding and period estimation

When folding the time series to integrated pulse profile, each pulse period has to be aligned according to our estimated local pulse. If the period estimate is not accurate, the peak position of the pulse profile in one pulse phase will drift. The resulting integrated pulse profile is distorted. However, as the single pulse is always hard to be observed, instead of observing the peak pulse position of each single pulse, we proposed segment folding to estimate the pulse period.

In segment folding, we first fold the time-series by short segments to make sure that the integrated pulse is discernible. Then by comparing the integrated profiles of several continuous segments, the drifting direction of peak position can be observed to decide whether the period is correct. As shown in Fig. 6(a), if the folding period is smaller than the correct period, the peak positions of segment-folded pulse profiles will drift to right, and as shown in Fig. 6(b), if the folding period is larger than the correct period, the peak positions will drift to left. When the folding period is exactly the correct pulse period, the peak positions are all aligned as shown in Fig. 7. According to this fact, the peak position detector can provide feedback on how to adjust the estimate of the pulse period.

D. PPS generation and precision analysis

With local period estimated, the standard PPS signal can be generated using the local clock according to the following relationship

$$1\text{s standard time} = \frac{P_l}{P_s} \times 1\text{s local time} \quad (6)$$

If the local time used by the Analog-to-Discrete Converter (ADC) is generated by the crystal oscillator with frequency f_0, the PPS signal is generated every $\frac{P_l}{P_s} f_0$ oscillator periods.

Let us denote the error between estimated local period and correct local period as $\Delta P \doteq \hat{P}_l - P_l$. Peak position of the intensity would drift ΔP per period if $\Delta P \neq 0$. For the digital signals with sample period t_{smp}, the drift will be noticeable when larger than t_{smp}. As a result, the smallest error that could be detected with the total process time t_{total} would be

$$\Delta P = t_{smp} \times \frac{P_l}{t_{total}} \quad (7)$$

and the minimum achievable estimation error rate is

$$\frac{\Delta P}{P_l} = \frac{t_{smp}}{t_{total}} \quad (8)$$

When using the estimated local period to generate the standard PPS signal, the error is

$$\Delta t = \frac{\Delta P}{P_l} \times 1\text{s} = \frac{t_{smp}}{t_{total}} \times 1\text{s} \quad (9)$$

Either increasing the sampling rate or prolonging the total process time can decrease the PPS error.

IV. CASE STUDY

In the last section, we use ten minutes' continuous observation data of the millisecond pulsar, J1939+2134, to verify the whole process procedure. J1939+2134 is one of the fastest rotating pulsars that has 1.557ms period, and its period is very stable over 30 years' observation. The observation data used here are the raw voltages out from the ADC recorded by the Very Large Array (VLA) radio telescope of National Radio Astronomy Observatory (NRAO). Table I presents the important facts about this pulsar and the raw voltage data.

In PFB part, the data are separated into $P = 1024$ filterbank channels. With its known DM, de-dispersion is implemented as shown in Fig. 4. With spectrum analysis, the comb-like spectra

TABLE I
FACTS OF J1939+2134 AND ITS OBSERVATION DATA

Facts of pulsar J1939+2134		
Pulsar Period	1.557806561	ms
Dispersion Measure	71.0237	$cm^{-3}pc$

Facts of the observation data		
Center frequency	1408	MHz
Observation bandwidth	32	MHz
Sampling intervals	15.625	ns
Total observation time	599.5	s

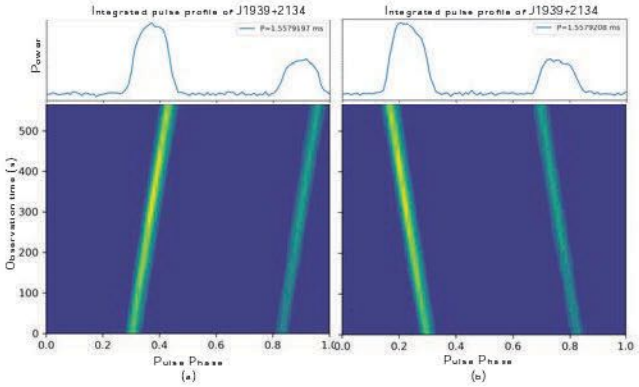

Fig. 6. Segment folding with periods smaller or larger than the correct period

of the periodic pulse signal can be observed as shown in Fig. 5, and the coarse estimate of local period is $\hat{P}_l = 1.557922$ms. Dividing the observation time to 20 segments, segment folding is implemented for each segment. When integrated with period that is smaller or larger than the correct period, the results of segment folding are shown in Fig. 6, which show drifting peak positions. When integrated with the right period, the result of segment folding is shown in Fig. 7, which shows that the peak positions of each segment is well-aligned. Through the iteration between segment folding and fine period estimator, the more accurate estimate of the local period is $\hat{P}_l = 1.557920256$ms.

As in this case, the total process time is 599.5 second and the sampling period after PFB is 16μs, so the minimum achievable error in PPS signal is

$$\Delta t = 26.69\text{ns}. \tag{10}$$

If the total process time is prolonged, the precision can be further improved.

V. CONCLUSION

While GPS signals are serving as the timing source of WAMS, pulsars can be an alternative and complementary timing source. Pulsar observation data can not be directly used for timing. The periodic pulse signals that the pulsars emit are undermined by dispersion, interference and noise. In this paper, a basic and practical algorithm is proposed to process the pulsar observation data and to generate standard timing signals for WAMS. Incoherent dispersion is used to mitigate pulse signal dispersion caused by space media. Spectrum

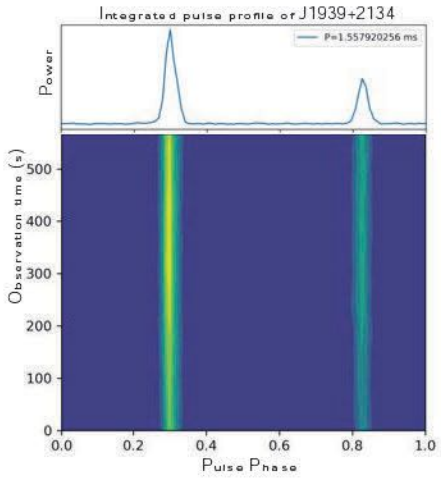

Fig. 7. Segment folding with the correct period

analysis can obtain the coarse estimate of the pulse period and segment folding can obtain the fine estimate of the pulse period. Standard PPS signal is generated according to the estimated pulse period and its accuracy is analyzed. The error of the generated PPS signal is related to the total observation time and the sampling period, and case study shows that the PPS error could be less than 100ns, which satisfies the demand for the timing source of WAMS. Given the facts that pulsars are highly stable clocks and can be observed worldwide, pulsars can serve as an accurate and reliable timing source for WAMS with our proposed method.

REFERENCES

[1] T. Bi, J. Guo, K. Xu, L. Zhang, and Q. Yang, "The impact of time synchronization deviation on the performance of synchrophasor measurements and wide area damping control," *IEEE Transactions on Smart Grid*, vol. 8, no. 4, pp. 1545–1552, 2016.

[2] J. Chai, Y. Liu, J. Guo, L. Wu, D. Zhou, W. Yao, Y. Liu, T. King, J. R. Gracia, and M. Patel, "Wide-area measurement data analytics using FNET/GridEye: A review," in *2016 Power Systems Computation Conference (PSCC)*. IEEE, 2016, pp. 1–6.

[3] R. S. Singh, H. Hooshyar, and L. Vanfretti, "Assessment of time synchronization requirements for phasor measurement units," in *2015 IEEE Eindhoven PowerTech*. IEEE, 2015, pp. 1–6.

[4] Z. Zhang, S. Gong, A. D. Dimitrovski, and H. Li, "Time synchronization attack in smart grid: Impact and analysis," *IEEE Transactions on Smart Grid*, vol. 4, no. 1, pp. 87–98, 2013.

[5] J. Zhao, Y. Liu, Y. Liu, P. L. Fuhr, T. King, H. Yin, L. Zhan, M. Morales-Rodriguez, W. Yao *et al.*, "Pulsar based timing synchronization method and system," Oct. 31 2019, uS Patent App. 16/397,687.

[6] Y. Yin, He amd Liu, P. Fuhr, M. Morales, M. Morganti, W. Monday, J. Richards, and S. Rooke, "Pulsar based alternative timing source for grid synchronization and operation," *accepted by IEEE Access*, 2020.

[7] D. R. Lorimer and M. Kramer, *Handbook of Pulsar Astronomy*, 2004, vol. 4.

[8] W. Van Straten, M. Bailes, M. Britton, K. S R, S. Anderson, R. Manchester, and J. Sarkissian, "A test of general relativity from the three-dimensional orbital geometry of a binary pulsar," *Nature*, vol. 412, no. 6843, pp. 158–160, 2001.

[9] R. Manchester, G. Hobbs, M. Bailes, W. Coles, W. Van Straten, M. Keith, R. Shannon, N. Bhat, A. Brown, S. Burke-Spolaor *et al.*, "The parkes pulsar timing array project," *Publications of the Astronomical Society of Australia*, vol. 30, 2013.

[10] Austria Telescope National Facility. The ATNF pulsar database. [Online]. Available: https://www.atnf.csiro.au/research/pulsar/psrcat